arXiv:1605.06999v1 [astro-ph.GA] 23 May 2016

A Tale of Three Galaxies: A "Clumpy" View of the Spectroscopically Anomalous Galaxies IRAS F10398+1455, IRAS F21013-0739 and SDSS J0808+3948

Yanxia Xie[*a,b,c,*], Robert Nikutta[*d], Lei Hao[*a], Aigen Li[*b]

[a]*Shanghai Astronomical Observatory, Chinese Academy of Sciences, 80 Nandan Road, Shanghai 200030, China*
[b]*Department of Physics and Astronomy, University of Missouri, Columbia, MO 65211, USA*
[c]*Kavli Institute for Astronomy and Astrophysics, Peking University, Beijing 100871, China*
[d]*Instituto de Astrofísica, Pontificia Universidad Católica de Chile, 306, Santiago 22, Chile*

Abstract

We investigate the dust properties in three spectroscopically anomalous galaxies (IRAS F10398+1455, IRAS F21013-0739 and SDSS J0808+3948). Their *Spitzer*/IRS spectra are characterized by a steep ∼5–8 μm emission continuum, strong emission bands from polycyclic aromatic hydrocarbon (PAH) molecules, and prominent 10 μm silicate emission. The steep ∼5–8 μm continuum and strong PAH emission features suggest the presence of starbursts, while the silicate emission is indicative of significant heating from AGNs. The simultaneous detection of these two observational properties has rarely been reported on galactic scale. We employ the PAHFIT software to estimate their starlight contributions, and the CLUMPY model for the components contributed by the AGN tori. We find that the CLUMPY model is generally successful in explaining the overall dust infrared emission, although it appears to emit too flat at the ∼5–8 μm continuum to be consistent with

[*]Corresponding authors.
Email addresses: yanxia.xie@pku.edu.cn (Yanxia Xie[*]), robert.nikutta@gmail.com (Robert Nikutta[*]), haol@shao.ac.cn (Lei Hao[*]), lia@missouri.edu (Aigen Li[*])

that observed in IRAS F10398+1455 and IRAS F21013-0739. The flat ∼5–8 μm continuum calculated from the CLUMPY model could arise from the adopted specific silicate opacity of Ossenkopf et al. (1992) which exceeds that of the Draine & Lee (1984) "astronomical silicate" by a factor up to 2 in the ∼5–8 μm wavelength range. Future models with a variety of dust species incorporated in the CLUMPY radiation transfer regime are needed for a thorough understanding of the dust properties of these spectroscopically anomalous galaxies.

Keywords: Infrared, Extinction, Dust, Model

1. Introduction

Dust is a ubiquitous feature of the cosmos. It is present in a wide variety of astrophysical systems, including active galactic nuclei (AGNs) and starburst galaxies (see Wang et al. 2014). Amorphous silicates and some form of carbonaceous materials (e.g., graphite, amorphous carbon, and hydrogenated amorphous carbon) are thought to be the two dominant cosmic dust species. Silicate dust reveals its presence in AGNs and starbursts through the 9.7 and 18 μm spectral features which respectively arise from the Si–O stretching and O–Si–O bending modes (e.g., see Henning 2010).

In AGNs, some dust is hot enough to generate a strong, *flat* emission continuum in the ∼5–8 μm wavelength range when the observed flux F_ν at frequency ν is plotted against wavelength λ, making it an effective diagnostic tool to distinguish AGN-dominated galaxies from starburst-dominated galaxies (e.g., see Laurent et al. 2000, Nardiniet al. 2008). In addition to silicate dust, polycyclic aromatic hydrocarbon (PAH) molecules also display rich emission bands in the mid infrared (IR; Tielens 2008). These features are usually very weak or absent in AGNs because PAHs are believed to have been destroyed by the harsh radiation field of AGNs (e.g., see Roche et al. 1991, Voit 1991, Siebenmorgen et al. 2004; but also see Alonso-Herrero et al. 2014). The 3.4 μm C–H stretching absorption feature is also detected in AGNs which indicates the presence of aliphatic, chain-like hydrocarbon dust in AGNs (e.g., see Imanishi et al. 1997, Mason et al. 2004).

Compared to AGNs, starburst galaxies commonly display a low, *red* ∼5–8 μm emission continuum, strong PAH emission features and silicate *absorption* features (e.g., Brandl et al. 2006, Hao et al. 2007, Smith et al. 2007). Moreover, starbursts lack the 3.4 μm absorption feature. This may be re-

lated to the fact that starbursts, particularly in their nuclear regions, are often heavily obscured by dust and ice. In the Milky Way, the 3.4 μm absorption feature is seen in the diffuse interstellar medium (ISM), but not in dense clouds where the 3.1 μm H_2O ice absorption feature is strong (see Pendleton & Allamandola 2002). Starbursts often exhibit strong H_2O ice absorption at 3.1 and 6.0 μm (e.g., see Spoon et al. 2004), while these ice features are not seen in AGNs where it is too hot for ice to survive against sublimation (see Li 2007).

Very recently, Xie et al. (2014, hereafter paper I) studied the $\sim$5–40 μm IR spectra of IRAS F10398+1455, IRAS F21013-0739, and SDSS J0808+3948 obtained with the *Infrared Spectrograph* (IRS) on board the *Spitzer Space Telescope* (Houck et al. 2004). They found that the IR spectra of these galaxies are *anomalous*. Their spectra, on one hand, resemble those of AGN in the sense that the silicate features in these galaxies are seen in *emission*; however, they also exhibit strong PAH emission features which are usually absent in AGNs that show similar silicate emission strengths as in these three galaxies (e.g., see Spoon et al. 2007). On the other hand, they are like starbursts in the sense that the $\sim$5–8 μm emission continua of these galaxies steeply rise with wavelength λ, and they show strong PAH emission features. The silicate features seen in *emission* in these galaxies are often seen in *absorption* in starbursts. Furthermore, the *steep* $\sim$5–8 μm emission continuum seen in these galaxies is much *flatter* in AGNs (see Figure 2). Let $\alpha = d\ln F_\nu / d\ln\lambda$ be the slope of the $\sim$5–8 μm emission continuum. On average, $\alpha \approx 0.8$ for quasars as derived from the averaged quasar spectrum (see Hao et al. 2007), while for IRAS F10398+1455, IRAS F21013-0739, and SDSS J0808+3948, $\alpha \approx 4.1$, 4.2, and 4.6, respectively. A detailed description of the spectral properties and a comparison of the *Spitzer*/IRS spectra of these three galaxies with that of typical starbursts and quasars can be found in Paper I.

Based on an extensive exploration of the multi-wavelength observational data, Y. Xie et al. (2016, in preparation) suggest that young/weak AGNs might be present in these three galaxies. The focus of this paper is to examine if the dust distribution in the circum-nuclear torus, and/or the viewing angle, play a role in generating such an anomalous mid-IR spectral energy distribution (SED). This paper is organized as follows. We describe the data in §2. In §3 we describe the CLUMPY torus model. The model-fitting to the observed IR emission is presented in §4. In §5 we discuss our results, and the major conclusions are summarized in §6. Throughout the paper, we

assume a cosmological model with $H_0 = 70\,h_{70}\,\mathrm{km\,s^{-1}\,Mpc^{-1}}$, $\Omega_m = 0.3$ and $\Omega_\wedge = 0.7$. $\mathrm{L}_\odot$ represents solar luminosity of $3.826 \times 10^{33}\,\mathrm{erg\,s^{-1}}$.

2. Observations and Data

These three galaxies were found in the *SDSS-Spitzer Spectral Atlas of Galaxies and AGNs* (hereafter S^{3}AGA, Hao et al. in preparation). We tabulate their basic properties in Table 1. The S^{3}AGA sample is constructed by cross-matching the 7th SDSS Data Release of main galaxy sample (Strauss et al. 2002) and the *Cornell AtlaS of Spitzer/IRS Sources* (CASSIS) catalog (Lebouteiller et al. 2011), including 598 galaxies with the SDSS and *Spitzer*/IRS position-difference smaller than 3″. In S^{3}AGA, the mid-IR spectra are restricted to those which have a full coverage in the *Spitzer*/IRS low-resolution wavelength interval of ∼5–38 μm. We visually exclude those that have poor quality spectra. The redshifts of these galaxies range from $z \approx 0.015$ to 0.36. So far, S^{3}AGA is the largest uniform sample[1] which combines optical and mid-IR data at z<0.4. Among this large sample, we have only identified three galaxies that exhibit such unique mid-IR dust features, implying that they are very rare in the local universe.

Table 1: Basic parameters for the three spectroscopically anomalous galaxies SDSS J0808+3948, IRAS F10398+1455, and IRAS F21013-0739.

Sources	R.A.	DEC.	Redshift	Program ID	$L_{\rm IR}$ ($\log_{10}\mathrm{L}_\odot$)
SDSS J0808+3948	08h08m44.27s	+39d48m52.36s	0.091	40444	10.84
IRAS F10398+1455	10h42m33.32s	+14d39m54.1s	0.099	40991	10.50
IRAS F21013−0739	21h03m58.75s	−07d28m02.5s	0.136	40444	10.53

The ∼5–8 μm continuum and the 9.7 and 18 μm silicate emission features result from dust grains that are heated by the AGN central engine. They attain an equilibrium temperature through the energy balance between the absorption of AGN UV photons and the emission of IR photons (see Li 2007).

[1]By uniform we mean the sample is constructed utilizing only the SDSS and Spitzer/IRS data and excluding the ISO or other IR data. This ensures that the systematic uncertainty of the whole sample is uniform.

The PAH emission features arise from PAH molecules which are stochastically heated by single stellar photons from their host galaxies (see Draine & Li 2001). Due to the differences in their emission mechanisms, chemical carriers and emitting regions, and to facilitate a detailed examination of the dust emission, we first remove the starlight, PAH emission features and the ionic emission lines from the *Spitzer*/IRS spectra of these galaxies. This requires an estimation of the dust emission continuum underneath the PAH and ionic emission lines. We approximate the continuum as a sum of starlight and blackbodies of different temperatures using the PAHFIT software (Smith et al. 2007) but with the addition of a warm silicate emission component to account for the 10 and 18 μm silicate emission features (see Paper I for details). The continuum determined in this way is hereafter referred to as "the PAHFIT continuum", we show our results in Figure 1. We are mostly interested in the residual dust emission obtained by subtracting the starlight, PAH and ionic emission lines from the observed *Spitzer*/IRS spectra. For illustration, we show in Figure 2 the residual dust emission of SDSS J0808+3948, IRAS F10398+1455 and IRAS F21013-0739, obtained by subtracting the starlight, PAH and ionic emission lines determined from the PAHFIT approach.

3. Dust Torus Model

Most of the circum-nuclear AGN dust emission is generated in the near-IR, presumably in a geometrically and optically thick torus that surrounds the central engine. The torus exists between $r_{\rm in}$ and $r_{\rm out}$, where $r_{\rm in}$ is the dust sublimation radius at which dust sublimates or evaporates (which is typically a fraction of a parsec and set by the illuminating luminosity), and $r_{\rm out}$ is the outer radius which is not well constrained. At $r_{\rm out}$, the torus either gradually fizzles, or possibly connects to regions that are dynamically related to the host galaxy. This outer radius is still the matter of investigation, both in the light of theoretical differences between the smooth-density torus models (e.g., see Pier & Krolik 1992, Granato & Danese 1994, Efstathiou & Rowan-Robinson 1995, Schartmann et al. 2005, Fritz et al. 2006), and the Clumpy torus models (e.g., see Nenkova et al. 2002, 2012a+b, Hönig et al. 2006, Schartmann et al. 2008, Stalevski et al. 2012, Siebenmorgen et al. 2015), but also because with ALMA it may be at last possible to determine $r_{\rm out}$ directly (see Nenkova et al. 2008b, and preliminary ALMA observations by García-Burillo et al. 2014).

Very-high angular resolution interferometry of nearby AGN suggests that the near- and mid-IR emission is spatially compact (e.g. Jaffe et al. 2004, Poncelet et al. 2006, Tristram et al. 2007, Raban et al. 2009, Burtscher et al. 2013), albeit this is only derived from simple geometric models of the 2D brightness distribution in the sky. The so-modeled mid-IR sizes, a few parsecs, suggest small tori indeed, which from the theory/modeling side favors clumpy dust distributions. Acknowledging that the specific choice of preferred model is a question beyond the scope of this paper, we decided on CLUMPY SEDs[2] for modeling the near- and mid-IR spectra of our three galaxies. CLUMPY, first introduced by Nenkova et al. (2002), and fully developed in Nenkova et al. (2002a,b), can compute the radiative transfer solution for an assumed axially-symmetric distribution of dusty clouds, each opaque with optical thickness τ_V, and illuminated by a central UV source. While probably all other models of clumpy tori are Monte-Carlo (MC) in nature, CLUMPY is a model with analytically computed statistical properties. It is therefore fast. The downside is that it computes the mean solution of all clumpy representations of a system at once, and can by design not generate a single clumpy view. The single-shot views in MC-based codes, on the other hand, can of course be on occasion very far from typical.

It is important to note that the gas and dust distributions in real systems are probably more complex than those in most simple 1D and 2D models. More recent 3D MC models allow for additional complexity, for instance by introducing a two-phase medium: a clumpy component, plus a smooth intra-cloud matter distribution (e.g. Stalevski et al. 2012, Siebenmorgen et al. 2015). Others have undertaken great efforts to compute in radiative-hydrodynamical simulations the distribution and flow of the interstellar molecular gas around a supermassive black hole, down to the very centers of AGNs (e.g. Wada & Norman 2002, Wada et al. 2009, Schartmann et al. 2010, Hopkins et al. 2012).

The formalism underlying the CLUMPY model was in detail described in Nenkova et al. (2002, 2008a, 2008b). We content ourselves with giving here the gist. In this model the AGNs torus is populated by dusty clouds, with matter-free space between them. Radiation can propagate unimpeded between the individually optically thick clouds. The visibility of the nucleus along the line-of-sight (LOS) to an external observer is probabilistic, and,

[2] www.clumpy.org

in stark contrast with smooth-density torus models, is governed not only by the torus angular width and the viewing angle, but also by the random clumpiness of the cloud distribution. An observer has a finite chance of seeing the unobscured nucleus even at edge-on views, if the photons generated in the central engine manage to avoid absorption by intervening torus clouds. Because clouds located at different position angles around the AGN show different phases of their hot and cool faces, an external observer always registers emission from a mix of different dust temperatures, originating from co-located regions around the AGN. That these different dust temperatures co-exist at the same distance from the central engine is a hallmark characteristic of clumpiness. It has been confirmed observationally in NGC 1068, using the *Mid-Infrared Interferometric Instrument* (MIDI) on the ESO's *Very Large Telescope Interferometer* (VLTI), where two co-located dust components at distinctly different temperatures of $\sim$800 K and $\sim$300 K have been found (Jaffe et al. 2004, Raban et al. 2009, Köhler & Li 2010). Notably, the hot component is missing in the resolved VLTI observations of the Circinus galaxy (Tristram et al. 2007, 2014). More recently, in a much more complete sample of AGNs observed with VLTI/MIDI, Burtscher et al. (2013) have modeled the observed radial brightness profiles with a resolved Gaussian plus an unresolved point-source. They find that the fractional contribution of the unresolved component exceeds $\sim$50% for 15 out of 23 detected AGNs. Even with the extremely high spatial resolution afforded by VLTI/MIDI, only two of the 20+ observable AGNs are close enough and luminous enough for their very central torus regions to be resolved. Burtscher et al. (2013) suspect that this may be the reason why so far only NGC 1068 has revealed a very hot dust component.

The simplest possible general makeup of an axially symmetric clumpy cloud distribution arguably requires no less than six free parameters. The radial torus size $r_{\rm out} = Y r_{\rm in}$ is a multiple of the scale-invariant dust sublimation radius $r_{\rm in}$, which is set only by the AGN luminosity, with Y a free parameter.

The mean number of clouds per radial ray in the equatorial plane clouds is N_0. For radial rays $90 - i$ degrees away from the equator the number of clouds along the line of sight (LOS) falls off as a Gaussian with width σ deg (measured from the equatorial plane). Our viewing angle i onto the system is measured from the torus axis. The local cloud number density falls off radially as $1/r^q$, with the power-law index q. Finally, the only property of a single cloud (in this minimal model) is its optical depth τ_V in the visual

band.

We consider a mixture of amorphous silicate (Ossenkopf et al. 1992) and graphite (Draine & Lee 1984), with a mass mixing ratio of 0.53 : 0.47. The dust grain size is assumed to follow a MRN-type power-law distribution for each dust species $dn/da \propto a^{-\beta}$, where the power-index β is fixed at 3.5, and the lower and upper cut-off sizes are taken to be $a_{\rm min} = 0.005\ \mu$m and $a_{\rm max} = 0.25\ \mu$m respectively (Mathis et al. 1977).

4. Results

In this section we fit the starlight, PAH- and gas-line-subtracted SEDs of the three galaxies, derived in §2, by using the CLUMPY model presented in §3. We then find the best-fit model parameters and their marginalized posteriors using the Bayesian Markov-Chain Monte Carlo (MCMC) SED fitting code developed by Nikutta et al. (2012). It performs a multi-dimensional interpolation of the model SEDs at the requested parameter values and wavelengths, and allows estimation of model parameters including their significance. As priors, we assume uniform probability density distributions for all parameters, in light of their unknown true properties.[3] The error bars for F10398+1455 and F21013-0739 are increased by a factor of 3 and 5 respectively, to aid the fitting algorithm which we think suffers otherwise under overly optimistic uncertainties on the data quality.

We tabulate the best-fit model parameters in Table 2 and illustrate the results in Figure 3. From the best-fitting model it is apparent that the torus-only model can explain the residual dust SED of SDSS J0808+3948 quite well. An exception is that the Si–O stretching feature of silicate dust peaks at $\sim$9.7 μm, while the model feature, owing to the silicate dust opacity used (Ossenkopf et al. 1992), peaks at $\sim$10.0 μm. This is curious, because when *Spitzer*, after long expectations, finally detected silicate emission features in type 1 AGNs (and in fact in some type 2s as well, e.g., see Mason et al. 2009, Nikutta et al. 2009), they all seemed to be flat-topped and their peaks shifted appreciably towards longer wavelengths (up to 11.6 μm in some cases). Researchers have been then calling for modified dust chemistry in AGN tori (e.g. Sturm et al. 2005) or argued that radiative transfer effects are the cause

[3]Note that we sample the viewing uniformly from $\cos(i) \in [0, 1]$ to ensure random distribution of orientations in the sphere of the sky.

of this shift (Nikutta et al. 2009, but also see Li et al. 2008, Smith et al. 2010).

For F10398+1455 and F21013-0739, the model predicts too flat a $\sim$5–8 μm continuum to be consistent with observations. In addition, as in SDSS J0808+3948 the model-calculated silicate emission feature for F10398+1455 and F21013-0739 also peaks at a wavelength longer than observed. These mismatches cannot likely be overcome by adjusting the cloud distribution and viewing angle.

5. Discussion

We have shown that no matter how we adjust the torus parameters, the dust IR emission SED calculated from the CLUMPY model is too high in the $\sim$5–8 μm wavelength range compared with the steep continuum of F10398+1455 and F21013-0739, and that the peak of the model silicate emission feature is at slightly longer wavelengths for all three sources.

One possible reason for the mismatches may lie in the specific interstellar dust properties that we used: the CLUMPY model assumes a mass mixture of 53% silicate dust and 47% graphite dust, with the optical constants of silicate and graphite respectively sourced from Ossenkopf et al. (1992) and Draine (2003). We note that among those AGNs exhibiting the silicate emission features, a vast majority have their "10 μm" feature peaking at a longer wavelength compared to that of the diffuse ISM (e.g., see Hao et al. 2005, Siebenmorgen et al. 2005, Sturm et al. 2005, Li et al. 2008, Mason et al. 2009, Smith et al. 2010, Shi et al. 2014). Nikutta et al. (2009) showed that the CLUMPY model with the Ossenkopf et al. (1992) silicates can explain AGNs with longward-shifted silicate peaks through radiative transfer effects in a clumpy medium (which are observed with peaks at up to 11.6 μm!). They also make the point that the features in systems with silicate *absorption* always seem to bottom at 9.7 μm. Others have obtained successful fits using more exotic dust chemistry (e.g. Jaffe et al. 2004, Sturm et al. 2005). The Ossenkopf et al. (1992) silicate actually has a longer peak position of $\sim$10.0 μm compared to that of the interstellar silicate profile which peaks at $\sim$9.7 μm (Kemper et al. 2004). However, for these three galaxies of interest in this paper, their silicate *emission* features all peak at $\sim$9.7 μm and are comparable to that of the interstellar silicate. Therefore, it is unavoidable for the CLUMPY model which is based on the Ossenkopf et al. (1992) silicate opacity to predict too long a peak wavelength for the silicate emission

feature. Moreover, the $\sim$1–8 μm continuum opacity of the Ossenkopf et al. (1992) silicate is higher than that of the Draine & Lee (1984) "astronomical silicate" by a factor up to 2. This explains the flat $\sim$5–8 μm continuum emission of the CLUMPY model: with the 9.7 and 18 μm silicate emission features remaining to be fitted, the Ossenkopf et al. (1992) silicate opacity would naturally result in a higher level of the $\sim$5–8 μm continuum emission than the Draine & Lee (1984) "astronomical silicate" (but also see Sirocky et al. 2008).

Also, the mismatch to the steep $\sim$5–8 μm continuum of F10398+1455 and F21013-0739 may be caused by the fixed mass ratio of silicate-to-graphite of $m_{\rm sil}/m_{\rm gra} = 1.13$. A higher $m_{\rm sil}/m_{\rm gra}$ ratio may lead to a steep $\sim$5–8 μm continuum. In Paper I, we have qualitatively discussed the possible dust properties that may account for the steep $\sim$5–8 μm continuum while exhibiting the prominent silicate emission feature in terms of dust composition, size and temperature. Based on the dust opacity characteristics presented in Figure 4 of Paper I, we proposed that sub-μm-sized, iron-poor silicate as well as the deficit of carbon dust could probably be responsible for the anomalous SEDs observed in these three galaxies.

In Xie et al. (2015, hereafter paper II) such dust properties have been explored in terms of a simple optically-thin model consisting of a mixture of warm and cold silicate dust, and warm and cold carbon dust. It was found that models consisting of "astronomical" silicate, amorphous olivine, or pyroxene, combined with amorphous carbon or graphite, are all capable of successfully fitting the observed IR emission. The dust temperature is the primary cause in regulating the steep $\sim$5–8 μm continuum and silicate emission, insensitive to the exact silicate or carbon dust mineralogy. More specifically, the temperature of the $\sim$5–8 μm continuum emitter (which is essentially carbon dust) of these galaxies is $\sim$250–400 K, much lower than that of typical quasars which is $\sim$640 K. The 9.7 μm emission feature constrains the silicate dust size to not exceed $\sim$1.0 μm (i.e., $a \lesssim 1.0\,\mu$m). The mass ratio of the warm carbon dust to the warm silicate dust ranges from $\sim$0.2 to $\sim$2.0, with a mean ratio of $\sim$0.98. Similarly, the mass ratio of the cold carbon dust to the cold silicate dust ranges from $\sim$0.34 to $\sim$2.0, with a mean ratio of $\sim$1.5. The total dust mass is dominated by the cold components, with the warm components only accounting for $< 0.15\%$ of the total dust mass.

To more effectively explore the dust properties of these three galaxies, one needs to incorporate these different dust compositions and mass ratios into

the CLUMPY radiation transfer model. In Nikutta et al. (2016, in preparation), we will investigate these dust characteristics with the CLUMPY model. Alternatively, the $\sim$5–8 μm continuum observed in the three galaxies might be affected by an optically thick dust disk (distinct from the clumpy component), which displays steeper $\sim$5–8 μm continuum emission in comparison with the clumpy models (see Siebenmorgen et al. 2015, Figure 5c).

To further explore if (and how) the $\sim$5–8 μm continuum emission is connected with the nature and distribution of the dust in a torus, we investigate the correlation between the slope of $\sim$5–8 μm continuum (defined as α, see §1) and the CLUMPY model parameters. We show our results in Figure 4; in each panel we also show the Kendall rank correlation coefficient (R) and significance (P) of correlation as well as the linear fit to the data set. It is apparent that α shows little correlation with Y, q, τ_V and i, while it appears that α is related to σ and N_0. The weak correlation between α and σ or N_0 is due to the fact that a *larger* σ or N_0 results in *more* obscuration in the inner torus and therefore overall *colder* dust emission.

6. Summary

We have modeled the *Spitzer*/IRS spectra of three spectroscopically anomalous galaxies (IRAS F10398+1455, IRAS F21013-0739 and SDSS J0808+3948) by decomposing them via PAHFIT, subtracting the starlight, PAH and atomline components, and then modeling the residual dust component with the CLUMPY torus model. The IR spectral characteristics of these galaxies are unique in the sense that they show silicate emission which is characteristic of AGNs, while they also show a steep $\sim$5–8 μm continuum and strong PAH emission features typical for starburst galaxies. In contrast, AGNs exhibit a *flat* emission continuum at $\sim$5–8 μm and lack the PAH emission features. The 9.7 and 18 μm silicate features seen in emission in these three galaxies are seen in absorption in starbursts.

We have investigated whether their anomalous SEDs could be explained by adjusting the dust cloud distribution and the viewing angle toward the AGNs torus. We find that the CLUMPY model is generally successful in explaining the overall dust IR emission, although it appears to emit too flat a $\sim$5–8 μm continuum to be consistent with that observed in IRAS F10398+1455 and IRAS F21013-0739. Also, the peak wavelength of the model silicate emission feature is too long compared with that observed in all three sources. We argue that the problem of the model-predicted longward-shifted silicate emis-

sion peak could be solved by incorporating different silicate species other than the Ossenkopf et al. (1992) silicate opacity, and the problem of the model-predicted flat $\sim$5–8 μm continuum could be solved by incorporating iron-poor silicate dust and/or a higher silicate-to-graphite mass ratio than that currently adopted in the CLUMPY model. Other than modifying the dust minerology, the presence of an optically thick dusty disk might also produce a steep slope of $\sim$5–8 μm continuum as seen in the three galaxies.

Acknowledgements

We thank all three referees for their very helpful comments. LH and XYX are partially supported by the 973 Program of China (2013CB834905, 2009CB824800), the Strategic Priority Research Program "The Emergence of Cosmological Structures" of Chinese Academy of Sciences (XDB09000000), the Shanghai Pujiang Talents Program (10pj1411800) and NSFC 11073040, 11173019. AL and XYX are supported in part by NSF AST-1311804 and NASA NNX14AF68G. RN acknowledges support by FONDECYT grant No. 3140436. The Cornell Atlas of *Spitzer*/IRS Sources (CASSIS) is a product of the Infrared Science Center at Cornell University, supported by NASA and JPL.

References

Allamandola, L.J., Tielens, A.G.G.M., Barker, J.R., 1985. Polycyclic Aromatic Hydrocarbons and the Unidentified Infrared Emission Bands – Auto Exhaust along the Milky Way. Astrophys. J. Lett. 290, L25-L28. doi: 10.1086/184435

Alonso-Herrero, A., Ramos Almeida, C., Esquej, P., et al. 2014. Nuclear 11.3 μm PAH emission in local active galactic nuclei. Mon. Not. R. Astron. Soc. 443, 2766-2782. doi: 10.1093/mnras/stu1293

Brandl, B. R., Bernard-Salas, J., Spoon, H. W. W., et al. 2006. The Mid-Infrared Properties of Starburst Galaxies from Spitzer-IRS Spectroscopy. Astrophys. J. 653, 1129-1144. doi: 10.1086/508849

Burtscher, L., Meisenheimer, K., Tristram, K. R. W., et al. 2013. A diversity of dusty AGN tori. Data release for the VLTI/MIDI AGN Large Program and first results for 23 galaxies. Astron. Astrophys. 558, A149. doi: 10.1051/0004-6361/201321890

Draine, B.T., 2003. Interstellar Dust Grains. Annu. Rev. Astron. Astrophys. J. 41, 241-289. doi: 10.1146/annurev.astro.41.011802.094840

Draine, B. T., & Li, A. 2001. Infrared Emission from Interstellar Dust. I. Stochastic Heating of Small Grains. Astrophys. J. 551, 807-824. doi: 10.1086/320227

Efstathiou, A., & Rowan-Robinson, M. 1995. Dusty discs in active galactic nuclei. Mon. Not. R. Astron. Soc. 273, 649. doi: 10.1093/mnras/273.3.649

Fritz, J., Franceschini, A., & Hatziminaoglou, E. 2006. Revisiting the infrared spectra of active galactic nuclei with a new torus emission model. Mon. Not. R. Astron. Soc., 366, 767. doi: 10.1111/j.1365-2966.2006.09866.x

García-Burillo, S., Combes, F., Usero, A., et al. 2014. Molecular line emission in NGC 1068 imaged with ALMA. I. An AGN-driven outflow in the dense molecular gas . Astron. Astrophys. 567, A125. doi: 10.1051/0004-6361/201423843

Granato, G. L., & Danese, L. 1994. Thick Tori around Active Galactic Nuclei – A Comparison of Model Predictions with Observations of the Infrared Continuum and Silicate Features. Mon. Not. R. Astron. Soc. 268, 235. doi: 10.1093/mnras/268.1.235

Hao, L., Spoon, H. W. W., Sloan, G. C., et al. 2005. The Detection of Silicate Emission from Quasars at 10 and 18 μm. Astrophys. J. Lett. 625, L75-L78. doi: 10.1086/431227

Hao, L., Weedman, D. W., Spoon, H. W. W., et al. 2007. The Distribution of Silicate Strength in Spitzer Spectra of AGNs and ULIRGs. Astrophys. J. Lett. 655, L77-L80. doi: 10.1086/511973

Hao, L., Lyu, J.W., Xie, Y., 2016. in preparation.

Henning, T. 2010. Cosmic Silicates. Annu. Rev. Astron. Astrophys. J. 48, 21-46. doi: 10.1146/annurev-astro-081309-130815

Hönig, S. F., Beckert, T., Ohnaka, K., & Weigelt, G. 2006. Radiative transfer modeling of three-dimensional clumpy AGN tori and its application to NGC 1068. Astron. Astrophys. 452, 459. doi: 10.1051/0004-6361:20054622

Hopkins, P. F., Hayward, C. C., Narayanan, D., & Hernquist, L. 2012. The origins of active galactic nuclei obscuration: The 'torus' as a dynamical, unstable driver of accretion. Mon. Not. R. Astron. Soc. 420, 320. doi: 10.1111/j.1365-2966.2011.20035.x

Houck, J. R., Roellig, T. L., van Cleve, J., et al. 2004. The Infrared Spectrograph (IRS) on the Spitzer Space Telescope. Astrophys. J. Suppl. Ser. 154, 18-24. doi: 10.1086/423134

Imanishi, M., Terada, H., Sugiyama, K., et al. 1997. Spectroscopic Study of NGC 1068 in the 3 μm Band. Publ. Astron. Soc. Japan. 49, 69-73. doi: 10.1093/pasj/49.1.69

Jaffe, W., Meisenheimer, K., Röttgering, H. J. A., et al. 2004. The central dusty torus in the active nucleus of NGC 1068. Nature. 429, 47-49. doi: 10.1038/nature02531

Kemper, F., Vriend, W. J., & Tielens, A. G. G. M. 2004. The Absence of Crystalline Silicates in the Diffuse Interstellar Medium. Astrophys. J. 609, 826-837. doi: 10.1086/421339

Köhler, M., & Li, A. 2010. On the anomalous silicate absorption feature of the prototypical Seyfert 2 galaxy NGC1068. Mon. Not. R. Astron. Soc. 406, L6-L10. doi: 10.1111/j.1745-3933.2010.00870.x

Laurent, O., Mirabel, I. F., Charmandaris, V., et al. 2000. Mid-infrared diagnostics to distinguish AGNs from starbursts. Astron. Astrophys. 359, 887-899.

Lebouteiller, V., Barry, D. J., Spoon, H. W. W., et al. 2011. CASSIS: The Cornell Atlas of Spitzer/Infrared Spectrograph Sources. Astrophys. J. Suppl. Ser. 196, 8-20. doi: 10.1088/0067-0049/196/1/8

Li, A. 2007. Dust in Active Galactic Nuclei. In The Central Engine of Active Galactic Nuclei (ASP Conf. Ser. 373), ed. L. C. Ho & J.-M. Wang (San Francisco, CA: ASP), 561-572

Li, M. P., Shi, Q. J., & Li, A. 2008. On the anomalous silicate emission features of active galactic nuclei: a possible interpretation based on porous dust. Mon. Not. R. Astron. Soc. 391, L49-L53. doi: 10.1111/j.1745-3933.2008.00553.x

Mason, R. E., Wright, G., Pendleton, Y., & Adamson, A. 2004. Hydrocarbon Dust Absorption in Seyfert Galaxies and Ultraluminous Infrared Galaxies. Astrophys. J. 613, 770-780. doi: 10.1086/423316

Mason, R. E., Levenson, N. A., Shi, Y., et al. 2009. The Origin of the Silicate Emission Features in the Seyfert 2 Galaxy NGC 2110. Astrophys. J. Lett. 693, L136. doi: 10.1088/0004-637X/693/2/L136

Mathis, J. S., Rumpl, W., & Nordsieck, K. H. 1997. The size distribution of interstellar grains. Astrophys. J. 217, 425. doi: 10.1086/155591

Nardini, E., Risaliti, G., Salvati, M., et al. 2008. Spectral decomposition of starbursts and active galactic nuclei in 5–8 μm Spitzer-IRS spectra of local ultraluminous infrared galaxies. Mon. Not. R. Astron. Soc. 385, L130-L134. doi: 10.1111/j.1745-3933.2008.00450.x

Nikutta, R., Elitzur, M., & Lacy, M. 2009. On the 10 μm Silicate Feature in Active Galactic Nuclei. Astrophys. J. 707, 1550-1559. doi: 10.1088/0004-637X/707/2/1550

Nikutta, R., 2012. Obscuration in Active Galactic Nuclei. PHD thesis, University of Kentucky.
url: http://uknowledge.uky.edu/physastron_etds/8/

Nikutta, R., Xie, Y., Li, A., & Hao, L., 2016. in preparation.

Nenkova, M., Ivezić, Ž., & Elitzur, M. 2002. Dust Emission from Active Galactic Nuclei. Astrophys. J. Lett. 570, L9-L12. doi: 10.1086/340857

Nenkova, M., Sirocky, M. M., Ivezić, Ž., & Elitzur, M. 2008a. AGN Dusty Tori. I. Handling of Clumpy Media. Astrophys. J. 685, 147-159. doi: 10.1086/590482

Nenkova, M., Sirocky, M. M., Nikutta, R., Ivezić, Ž., & Elitzur, M. 2008b. AGN Dusty Tori. II. Observational Implications of Clumpiness. Astrophys. J. 685, 160-180. doi: 10.1086/590483

Ossenkopf, V., Henning, T., & Mathis, J. S. 1992. Constraints on cosmic silicates. Astron. Astrophys. 261, 567-578.

Pendleton, Y.J., Allamandola, L.J., 2002. The Organic Refractory Material in the Diffuse Interstellar Medium: Mid-Infrared Spectroscopic Constraints. Astrophys. J. Suppl. Ser. 138, 75-98. doi: 10.1086/322999

Pier, E. A., & Krolik, J. H. 1992. Infrared spectra of obscuring dust tori around active galactic nuclei. I - Calculational method and basic trends. Astrophys. J. 401, 99. doi: 10.1086/172042

Poncelet, A., Perrin, G., & Sol, H. 2006. A new analysis of the nucleus of NGC 1068 with MIDI observations. Astron. Astrophys. 450, 483. doi: 10.1051/0004-6361:20053608

Raban, D., Jaffe, W., Röttgering, H., Meisenheimer, K., & Tristram, K. R. W. 2009. Resolving the obscuring torus in NGC 1068 with the power of infrared interferometry: revealing the inner funnel of dust. Mon. Not. R. Astron. Soc. 394, 1325-1337. doi: 10.1111/j.1365-2966.2009.14439.x

Roche, P. F., Aitken, D. K., Smith, C. H., et al. 1991. An atlas of mid-infrared spectra of galaxy nuclei. Mon. Not. R. Astron. Soc. 248, 606. doi: 10.1093/mnras/248.4.606

Schartmann, M., Meisenheimer, K., Camenzind, M., Wolf, S., & Henning, T. 2005. Towards a physical model of dust tori in Active Galactic Nuclei. Radiative transfer calculations for a hydrostatic torus model. Astron. Astrophys. 437, 861. doi: 10.1051/0004-6361:20042363

Schartmann, M., Meisenheimer, K., Camenzind, M., et al. 2008. Three-dimensional radiative transfer models of clumpy tori in Seyfert galaxies. Astron. Astrophys. 482, 67. doi: 10.1051/0004-6361:20078907

Schartmann, M., Burkert, A., Krause, M., et al. 2010, Mon. Not. R. Astron. Soc., 403, 1801

Shi, Y., Rieke, G. H., Ogle, P. M., Su, K. Y. L., & Balog, Z. 2014. Infrared Spectra and Photometry Of Complete Samples of Palomar-Green and Two Micron All Sky Survey Quasars. Astrophys. J. Suppl. Ser. 214, 23-39. doi: 10.1088/0067-0049/214/2/23

Siebenmorgen, R., Krügel, E., & Spoon, H. W. W. 2004. Mid-infrared emission of galactic nuclei. TIMMI2 versus ISO observations and models. Astron. Astrophys. 414, 123-139. doi: 10.1051/0004-6361:20031633

Siebenmorgen, R., Haas, M., Krügel, E., & Schulz, B. 2005. Discovery of 10 μm silicate emission in quasars. Evidence of the AGN unification scheme. Astron. Astrophys. 436, L5-L8. doi: 10.1051/0004-6361:200500109

Siebenmorgen, R., Heymann, F., & Efstathiou, A. 2015. Self-consistent two-phase AGN torus models. SED library for observers. Astron. Astrophys. 583, A120. doi: 10.1051/0004-6361/201526034

Sirocky, M. M., Levenson, N. A., Elitzur, M., et al. 2008. Silicates in Ultraluminous Infrared Galaxies. Astrophys. J. 678, 729-743. doi: 10.1086/586727

Smith, J. D. T., Draine, B. T., Dale, D. A., et al. 2007. The Mid-Infrared Spectrum of Star-forming Galaxies: Global Properties of Polycyclic Aromatic Hydrocarbon Emission. Astrophys. J. 656, 770-791. doi: 10.1086/510549

Smith, H. A., Li, A., Li, M. P., et al. 2010. Anomalous Silicate Dust Emission in the Type 1 Liner Nucleus of M81. Astrophys. J. 716, 490-503. doi: 10.1088/0004-637X/716/1/490

Spoon, H. W. W., Armus, L., Cami, J., et al. 2004. Fire and Ice: Spitzer Infrared Spectrograph (IRS) Mid-Infrared Spectroscopy of IRAS F00183-7111. Astrophys. J. Suppl. Ser. 154, 184-187. doi: 10.1086/422813

Spoon, H. W. W., Marshall, J. A., Houck, J. R., et al. 2007. Mid-Infrared Galaxy Classification Based on Silicate Obscuration and PAH Equivalent Width. Astrophys. J. 654, L49-L52. doi: 10.1086/511268

Stalevski, M., Fritz, J., Baes, M., Nakos, T., & Popović, L. Č. 2012. 3D radiative transfer modelling of the dusty tori around active galactic nuclei as a clumpy two-phase medium. Mon. Not. R. Astron. Soc. 420, 2756. doi: 10.1111/j.1365-2966.2011.19775.x

Sturm, E., Schweitzer, M., Lutz, D., et al. 2005. Silicate Emissions in Active Galaxies: From LINERs to QSOs. Astrophys. J. Lett. 629, L21-L23. doi: 10.1086/444359

Tielens, A. G. G. M. 2008. Interstellar Polycyclic Aromatic Hydrocarbon Molecules. Annu. Rev. Astron. Astrophys. J. 46, 289-337. doi: 10.1146/annurev.astro.46.060407.145211

Tristram, K. R. W., Meisenheimer, K., Jaffe, W., et al. 2007. Resolving the complex structure of the dust torus in the active nucleus of the Circinus galaxy. Astron. Astrophys. 474, 837. doi: 10.1051/0004-6361:20078369

Tristram, K. R. W., Burtscher, L., Jaffe, W., et al. 2014. The dusty torus in the Circinus galaxy: a dense disk and the torus funnel. Astron. Astrophys. 563, A82. doi: 10.1051/0004-6361/201322698

Voit, G. M. 1991. X-ray irradiation of interstellar grains in active galaxies - Evaporation and infrared spectra. Astrophys. J. 379, 122. doi: 10.1086/170490

Wada, K., & Norman, C. A. 2002. Obscuring Material around Seyfert Nuclei with Starbursts. Astrophys. J. Lett. 566, L21. doi: 10.1086/339438

Wada, K., Papadopoulos, P. P., & Spaans, M. 2009. Molecular Gas Disk Structures Around Active Galactic Nuclei. Astrophys. J. 702, 63. doi: 10.1088/0004-637X/702/1/63

Wang, M. L., Li, A., Xiang, F. Y., et al. 2014. Dust in active galactic nuclei. Scientia Sinica Physica, Mechanica & Astronomica 44, 771. doi: 10.1360/SSPMA2013-00109

Xie, Y., Hao, L., & Li, A. 2014. A Tale of Three Galaxies: Anomalous Dust Properties in IRAS F10398+1455, IRAS F21013-0739, and SDSS J0808+3948. Astrophys. J. Lett. 794, L19-L24. doi: 10.1088/2041-8205/794/2/L19

Xie, Y., Li, A., Hao, L., & Nikutta, R. 2015. A Tale of Three Galaxies: Deciphering the Infrared Emission of the Spectroscopically Anomalous Galaxies IRAS F10398+1455, IRAS F21013-0739, and SDSS J0808+3948. Astrophys. J. 808, 145. doi: 10.1088/0004-637X/808/2/145

Xie, Y., Hao, L., Charmandaris, V., Diaz-Santos, T., Nikutta, R., 2016. in preparation.

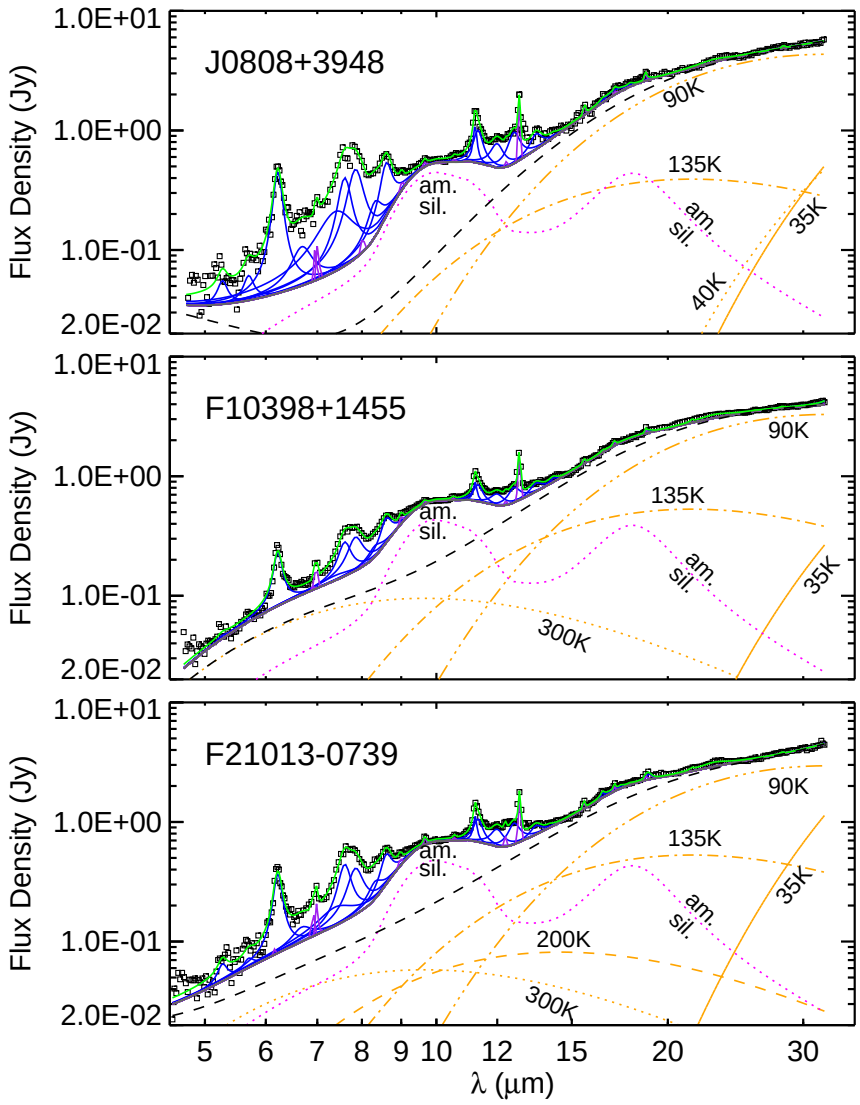

Figure 1: Fitting the *Spitzer*/IRS spectra of SDSS J0808+3948, IRAS F10398+1455, and IRAS F21013-0739 with PAHFIT. The IRS spectra (open black squares) are fitted with a combination of PAHs (solid blue lines), ionic lines (solid purple lines), warm silicate emission (dotted magenta line), modified blackbodies of different temperatures (orange lines) and starlight. The sum of the modified blackbodies and starlight represents the continuum underneath the PAH and silicate features (black dashed line). In each panel, the PAH features are fitted with Drude profiles and the ionic lines are fitted with Gaussian functions.

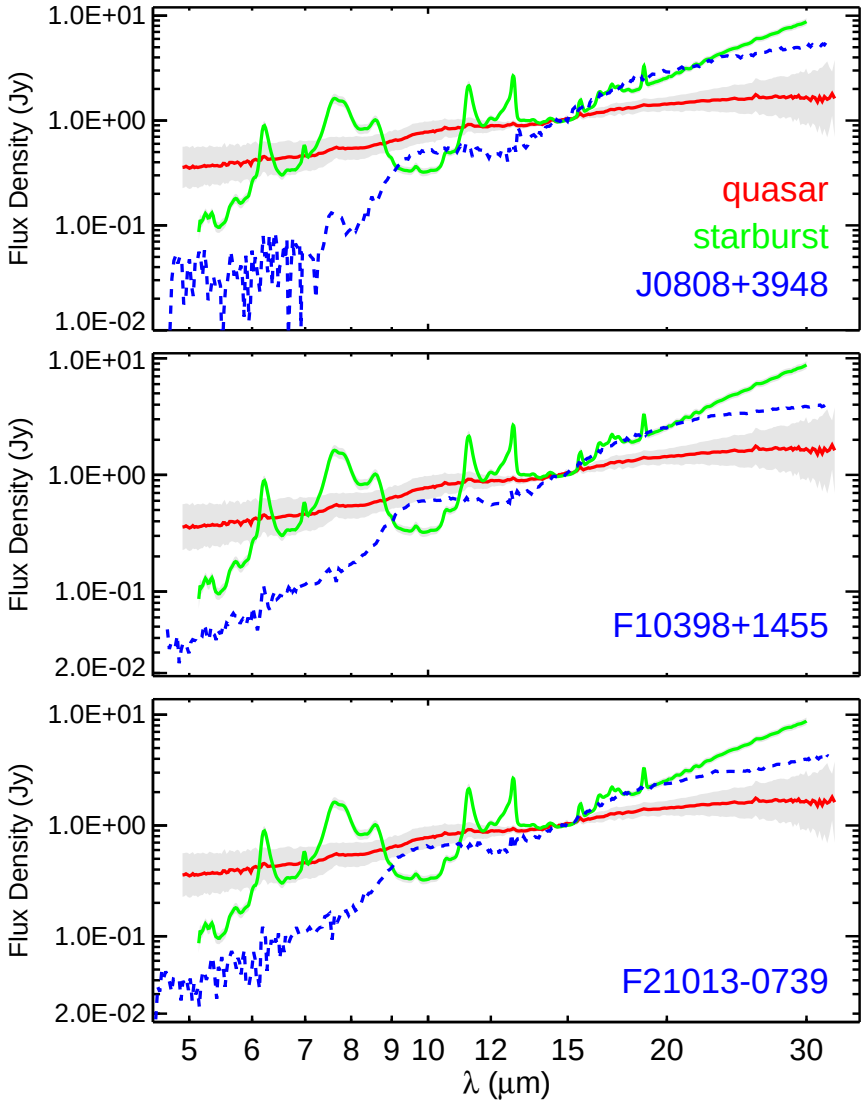

Figure 2: The "residual" dust emission of SDSS J0808+3948, IRAS F10398+1455, and IRAS F21013-0739 obtained by subtracting from the *Spitzer*/IRS spectrum the starlight, PAH and ionic emission lines determined via PAHFIT (blue dashed line). In each panel, we also show the average IRS spectrum of quasars (red line, Hao et al. 2007), and starbursts (green line, Brandl et al. 2006) for comparison. All spectra are normalized at $\lambda = 15\,\mu$m.

Table 2: Parameters inferred from fitting with the CLUMPY models

Parameter →	Y		σ		q		τ_V		i		N_0	
Source ↓	MAP	median	MAP	median	MAP	median	MAP	median	MAP	median	MAP	median
SDSS J0808+3948	20.93	$22.41^{+1.59}_{-1.58}$	29.76	$30.21^{+4.96}_{-2.39}$	0.00	$0.18^{+0.32}_{-0.18}$	300.00	$283.09^{+16.91}_{-31.42}$	90.00	$86.18^{+3.82}_{-5.18}$	13.80	$13.18^{+1.35}_{-2.38}$
IRAS F10398+1455	19.40	$19.42^{+1.41}_{-1.75}$	15.00	$15.34^{+1.49}_{-0.34}$	0.00	$0.01^{+0.09}_{-0.01}$	184.94	$185.93^{+7.74}_{-11.60}$	89.83	$89.34^{+0.66}_{-2.34}$	10.59	$10.82^{+0.91}_{-0.49}$
IRAS F21013−0739	22.84	$22.60^{+1.40}_{-1.77}$	18.58	$21.03^{+6.80}_{-4.20}$	0.31	$0.19^{+0.31}_{-0.19}$	300.00	$274.13^{+25.87}_{-32.13}$	75.42	$76.68^{+7.32}_{-4.68}$	15.00	$10.64^{+2.96}_{-3.11}$

Note: For each parameter, the first column indicates the maximum-a-posteriori (MAP) value, i.e. the combination of parameter values that simultaneously miximizes the likelihood. The second column indicates the median value of the parameter distribution (i.e. the 50th percentile of the cumulative distribution function, CDF), and the 1σ confidence interval (68.3% of the CDF around the median).

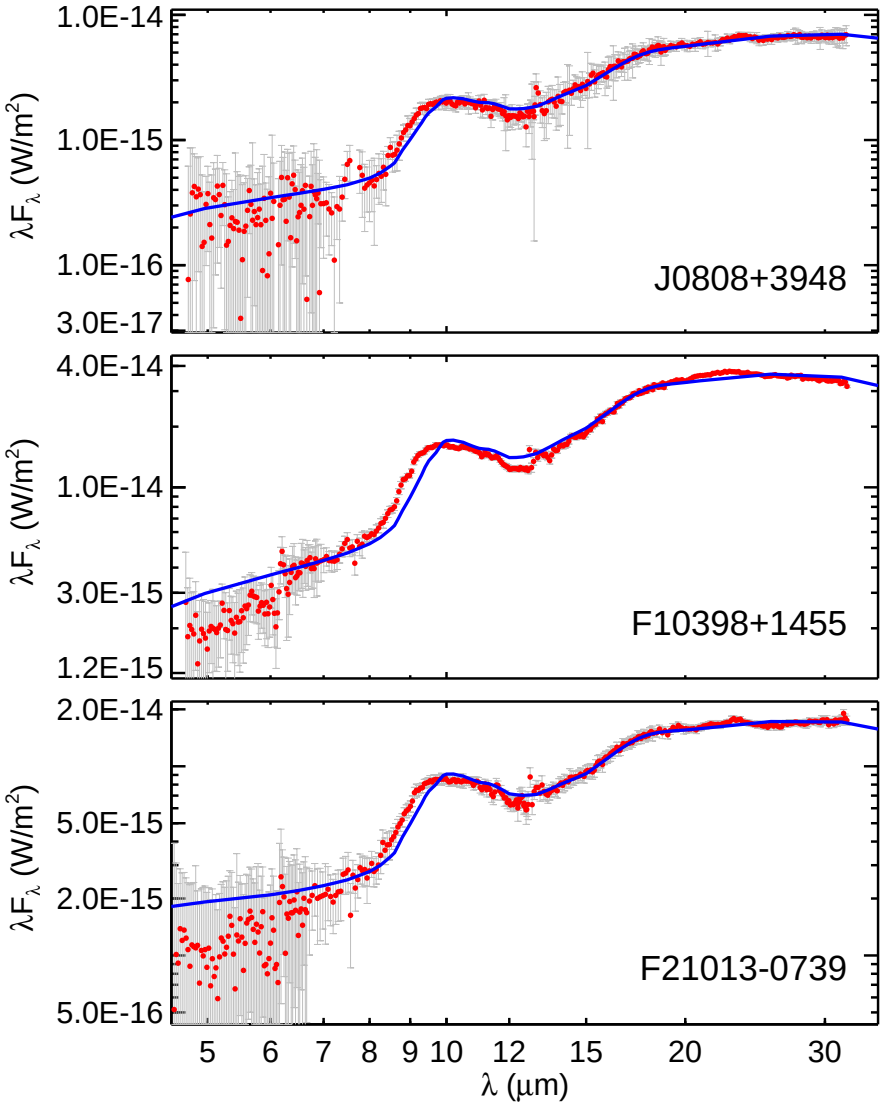

Figure 3: CLUMPY model-fits to the starlight, PAH- and gas-line-subtracted residual spectra of SDSS J0808+3948, IRAS F10398+1455 and IRAS F21013-0739 obtained in §2. In each panel, the red dots plot the observed data, and the error bars on the data points are shown with gray lines (for F10398+1455 and F21013-0739 they were multiplied by factors 3 and 5, respectively. For J0808+3948 they are the 1σ errors). The solid blue line shows the best fit derived from the CLUMPY model.

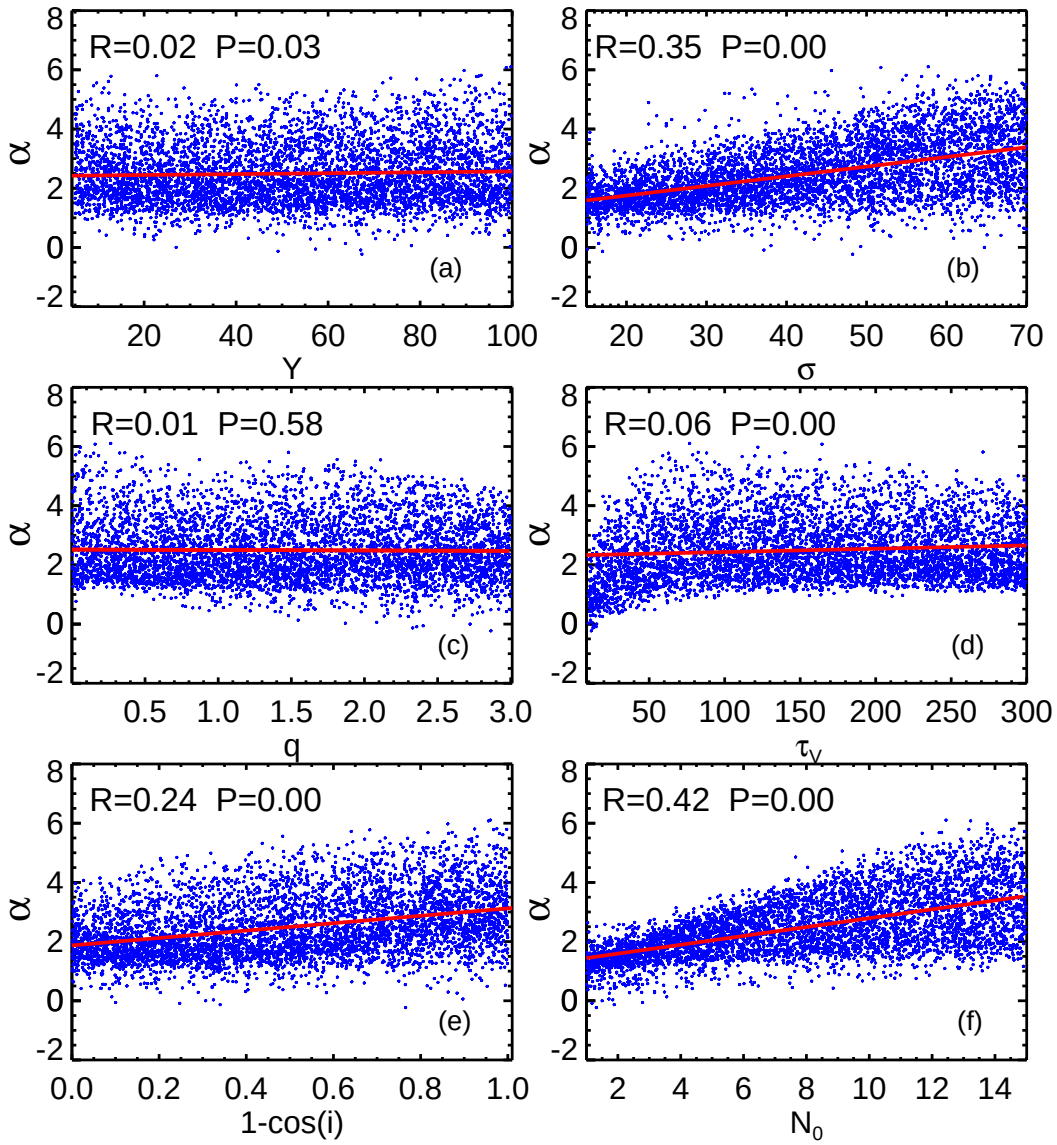

Figure 4: Correlation of $\alpha = d\ln F_\nu / d\ln\lambda$, the slope of the $\sim$5–8 μm emission continuum, with (a) $Y = r_{\rm out}/r_{\rm in}$, the ratio of the torus outer radius to the torus inner radius; (b) σ, the dispersion of the Gaussian function characterizing the cloud distribution in polar angle ("vertical thickness of the torus") (c) q, the index of the power-law radial distribution of the cloud number density ($\propto 1/r^q$); (d) τ_V, the optical depth of a single dust cloud in the visual band; (e) i, the viewing angle (defined as the angle between the LOS and the torus symmetry axis); and (f) N_0, the mean number of clouds per radial ray in the equatorial plane. While α shows little correlation with Y, q, τ_V and i, it appears that α weakly correlates with σ and N_0.